arXiv:0904.4346v2 [hep-ph] 12 Jun 2009

Mössbauer neutrinos in quantum mechanics and quantum field theory

Joachim Kopp[a]

Max–Planck–Institut für Kernphysik,
Postfach 10 39 80, 69029 Heidelberg, Germany

29 April 2009

Abstract

We demonstrate the correspondence between quantum mechanical and quantum field theoretical descriptions of Mössbauer neutrino oscillations. First, we compute the combined rate Γ of Mössbauer neutrino emission, propagation, and detection in quantum field theory, treating the neutrino as an internal line of a tree level Feynman diagram. We include explicitly the effect of homogeneous line broadening due to fluctuating electromagnetic fields in the source and detector crystals and show that the resulting formula for Γ is identical to the one obtained previously [1] for the case of inhomogeneous line broadening. We then proceed to a quantum mechanical treatment of Mössbauer neutrinos and show that the oscillation, coherence, and resonance terms from the field theoretical result can be reproduced if the neutrino is described as a superposition of Lorentz-shaped wave packet with appropriately chosen energies and widths. On the other hand, the emission rate and the detection cross section, including localization and Lamb-Mössbauer terms, cannot be predicted in quantum mechanics and have to be put in by hand.

1 Introduction

The possibility of exploiting the Mössbauer effect in weak interactions to enhance the small neutrino cross sections [2, 3, 4, 5, 6] has recently received considerable interest, both from the experimental side [5, 6, 7, 8] and from the theoretical side [1, 9, 10, 11, 12, 13, 14, 15, 16]. In the proposed experiment, neutrinos are emitted from ^{3}H atoms embedded into a metal crystal and absorbed by ^{3}He atoms embedded into a similar crystal. With very optimistic assumptions on the source activity (1 MCi), the fraction of recoilfree emissions and absorptions (0.28 each), and the achievable spectral line width ($\Delta E/E \sim 10^{-11}$ eV/18.6 keV $\sim 5{\cdot}10^{-16}$), it has been estimates that an event rate of 10^3 per day could be achieved for a detector containing 1 g of ^{3}He and placed at a baseline $L = 10$ m [6].[1] These events could be counted

[a]Email: jkopp@mpi-hd.mpg.de

[1]It has been suggested recently that it might even be possible to reach a line width of $\mathcal{O}(10^{-24}$ eV), corresponding to the natural line width of tritium decay [17, 18, 19]. This would imply an additional enhancement of the event rate by a factor of 10^{13}, allowing for smaller sources and detectors, or for longer baselines. However, the arguments given in [17, 18, 19] in favor of this additional enhancement have been disproven in ref. [20].

by observing the subsequent decays of the produced ^{3}H in the detector, or by chemically extracting and counting the number of produced ^{3}H atoms. However, it is far from clear whether the above experimental performance can be achieved in practice, and, in fact, the event rate may well be many orders of magnitude smaller [8], so that the question of whether a Mössbauer neutrino experiment can be realized in practice is still open.

In spite of this, Mössbauer neutrinos have already now proven to be an excellent test case for studying the quantum mechanics and quantum field theory of neutrino oscillations theoretically. In particular, their extremely small energy spread of $\mathcal{O}(10^{-11}$ eV) [7, 21] has led to the question whether a coherent emission and absorption of different neutrino mass eigenstates, which is a prerequisite for oscillations, is possible [11, 14]. Even though a detailed quantum field theoretical treatment, requiring no a priori assumptions on the neutrino wave function, shows that oscillations do occur in a Mössbauer neutrino experiment [1, 13], such an approach also reveals that Mössbauer neutrinos are special because many of the assumptions and approximations that are commonly made in the theoretical treatment of conventional neutrino oscillation experiments are invalid for them.

In this paper, we will use the example of Mössbauer neutrinos to discuss the correspondence between quantum mechanical and quantum field theoretical approaches to neutrino oscillations. In sec. 2, we will derive the combined rate of Mössbauer neutrino emission, propagation, and detection in quantum field theory (QFT). We will for the first time explicitly include homogeneous line broadening effects arising from fluctuating electromagnetic fields in the solid state crystals forming the Mössbauer source and detector, and we will show that, as anticipated in ref. [1], the result is identical to the one obtained for inhomogeneous line broadening due to crystal imperfections. We will then derive the same result from quantum mechanics (QM) in sec. 3, treating the neutrino as a wave packet. A comparison of the QFT and QM approaches will show that QM is inferior to QFT because more ad hoc assumptions are required, e.g. on the shape and width of the neutrino wave packets. If, however, all parameters are chosen appropriately in the QM formalism, the QFT result can be reproduced. In sec. 4, we will discuss our results and conclude.

2 Mössbauer neutrinos in quantum field theory and homogeneous line broadening

To compute the amplitude for Mössbauer neutrino production, propagation, and detection in QFT, we follow the formalism developed in [1] and consider the Feynman diagram shown in fig. 1. Here, the external lines correspond to the ^{3}H and ^{3}He *atoms* in the source (S) and the detector (D), while the internal line describes the propagating antineutrino. Since we are mainly interested in the phenomenology of Mössbauer neutrino oscillations, we avoid an explicit treatment of solid state binding forces and instead assume the external particles to reside in the ground states of simple harmonic oscillator potentials, with oscillator frequencies of the order of the Debye temperature $\Theta_D \sim 600$ K $\simeq 0.05$ eV of the respective crystals [6, 7]. It is known from the theory of the classical photon Mössbauer effect [22], that this model provides qualitatively correct results, even though it is, of course, insufficient for computing a precise prediction of the total event rate. If we denote the masses of the external particles by m_A ($A = \{\mathrm{H}, \mathrm{He}\}$), their average positions by $\mathbf{x}_B$ ($B = \{S, D\}$), the harmonic oscillator frequencies by $\omega_{A,B}$, and the ground state energies by $E_{A,B}$, the wave

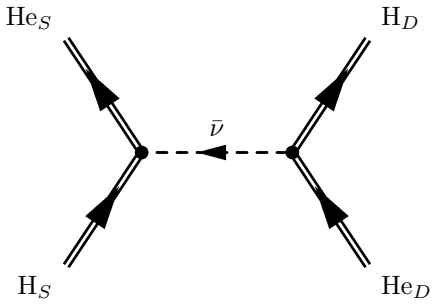

Figure 1: Feynman diagram for neutrino emission and absorption in the ^{3}H$-^3$He system.

functions corresponding to the external legs in fig. 1 are given by,

$$\psi_{A,B,0}(\mathbf{x},t) = \left[\frac{m_A\omega_{A,B}}{\pi}\right]^{\frac{3}{4}} \exp\left[-\frac{1}{2}m_A\omega_{A,B}|\mathbf{x}-\mathbf{x}_B|^2\right] e^{-iE_{A,B}t}\,. \tag{1}$$

Due to interactions of the atoms with their surroundings, $E_{A,B}$ will not be constant in time, but will fluctuate around the average zero point energy $E_{A,B,0} = m_A + \frac{1}{2}\omega_{A,B}$ [21, 23, 24, 25, 26]. These fluctuations are, for example, induced by random thermal spin flips of neighboring atoms. They are generally referred to as homogeneous line broadening effects because, as we will see below, they limit the achievable sharpness of the Mössbauer resonance. To describe homogeneous line broadening, we make the replacement [23]

$$e^{-iE_{A,B}t} \to e^{-iE_{A,B,0}t}\, f_{A,B}(t)\,, \tag{2}$$

in eq. (1), where

$$f_{A,B}(t) = \exp\left[-i\int_0^t dt'\left(E_{A,B}(t') - E_{A,B,0}\right)\right] \tag{3}$$

is integrated phase shift induced by the fluctuations of $E_{A,B}$. Note that this approach accounts only for homogeneous line broadening due to solid-state effects, but not for broadening due the natural line width. The latter effect (which is theoretically interesting, but completely negligible in the ^{3}H$-^3$He system) has been studied in detail in ref. [1]. The

transition amplitude corresponding to fig. 1, including the modulation factors (3), is

$$
\begin{aligned}
i\mathcal{A} = \int d^3x_1\, dt_1 \int d^3x_2\, dt_2 \left(\frac{m_{\rm H}\omega_{{\rm H},S}}{\pi}\right)^{\frac{3}{4}} \exp\left[-\frac{1}{2}m_{\rm H}\omega_{{\rm H},S}|\mathbf{x}_1-\mathbf{x}_S|^2\right] f_{{\rm H},S}(t_1)\, e^{-iE_{{\rm H},S}t_1} \\
\cdot \left(\frac{m_{\rm He}\omega_{{\rm He},S}}{\pi}\right)^{\frac{3}{4}} \exp\left[-\frac{1}{2}m_{\rm He}\omega_{{\rm He},S}|\mathbf{x}_1-\mathbf{x}_S|^2\right] f^*_{{\rm He},S}(t_1)\, e^{+iE_{{\rm He},S}t_1} \\
\cdot \left(\frac{m_{\rm He}\omega_{{\rm He},D}}{\pi}\right)^{\frac{3}{4}} \exp\left[-\frac{1}{2}m_{\rm He}\omega_{{\rm He},D}|\mathbf{x}_2-\mathbf{x}_D|^2\right] f_{{\rm He},D}(t_2)\, e^{-iE_{{\rm He},D}t_2} \\
\cdot \left(\frac{m_{\rm H}\omega_{{\rm H},D}}{\pi}\right)^{\frac{3}{4}} \exp\left[-\frac{1}{2}m_{\rm H}\omega_{{\rm H},D}|\mathbf{x}_2-\mathbf{x}_D|^2\right] f^*_{{\rm H},D}(t_2)\, e^{+iE_{{\rm H},D}t_2} \\
\cdot \sum_j \mathcal{M}^\mu_S \mathcal{M}^{\nu *}_D\, |U_{ej}|^2 \int \frac{d^4p}{(2\pi)^4} \exp\left[-ip_0(t_2-t_1)+i\mathbf{p}(\mathbf{x}_2-\mathbf{x}_1)\right] \\
\cdot \bar{u}_{e,S}\gamma_\mu(1-\gamma^5)\,\frac{i(\not{p}+m_j)}{p_0^2-\mathbf{p}^2-m_j^2+i\epsilon}\,(1+\gamma^5)\gamma_\nu u_{e,D}\,. \qquad (4)
\end{aligned}
$$

Here, m_j are the neutrino mass eigenvalues, U_{ej} are elements of the leptonic mixing matrix, and the nonrelativistic (i.e. momentum-independent) electron spinors are denoted by $u_{e,S}$ for the electron that is emitted in ^{3}H decay in the source, and by $u_{e,D}$ for the electron that is destroyed in the neutrino capture process in the detector. The matrix elements $\mathcal{M}^\mu_S$ and $\mathcal{M}^\mu_D$ are given by

$$
\mathcal{M}^\mu_{S,D} = \frac{G_F\cos\theta_c}{\sqrt{2}}\,\psi_e(R)\,\bar{u}_{\rm He}(M_V\,\delta^\mu_0 - g_A M_A\gamma^i\gamma^5\,\delta^\mu_i/\sqrt{3})u_{\rm H}\,\kappa^{1/2}_{S,D}\,, \qquad (5)
$$

where G_F is the Fermi constant, θ_c the Cabibbo angle, and $u_{A,B}$ (with $A=\{{\rm H},{\rm He}\}$, $B=\{S,D\}$ as before) are the non-relativistic ^{3}H and ^{3}He spinors. The vector and axial vector (or Fermi and Gamow-Teller) nuclear matrix elements are $M_V=1$ and $M_A\approx\sqrt{3}$, respectively [27, 28], and the axial-vector coupling constant is $g_A\simeq 1.25$. The quantity $\psi_e(R)$ gives the value of the anti-symmetrized atomic wave function of ^{3}He at the surface of the nucleus, while the factor

$$
\kappa_{S,D} = \left|\int \Psi_{Z=2,S,D}(\mathbf{r})^*\,\Psi_{Z=1,S,D}(\mathbf{r})\,d^3r\right|^2. \qquad (6)
$$

accounts for the fact that the spectator electron in bound state ^{3}H decay and induced orbital electron capture on ^{3}He changes from the $1s$ state of ^{3}H into the $1s$ state of ^{3}He, or vice-versa.

The spatial integrals in (4) yield a factor $\exp[-\mathbf{p}^2/2\sigma_p^2]\exp[i\mathbf{pL}]$, with the effective momentum uncertainty σ_p of the experiment defined by

$$
\frac{1}{\sigma_p^2} = \frac{1}{\sigma_{pS}^2}+\frac{1}{\sigma_{pD}^2} = \frac{1}{m_{\rm H}\omega_{{\rm H},S}+m_{\rm He}\omega_{{\rm He},S}}+\frac{1}{m_{\rm H}\omega_{{\rm H},D}+m_{\rm He}\omega_{{\rm He},D}}\,, \qquad (7)
$$

and with the baseline vector

$$\mathbf{L} = \mathbf{x}_D - \mathbf{x}_S \,. \tag{8}$$

To evaluate the three-momentum integral, we employ the Grimus-Stockinger theorem [29], which states that, for any three times continuously differentiable function $\psi(\mathbf{p})$ ($\mathbf{p} \in \mathbb{R}^3$), with ψ and all its first and second derivatives decreasing at least as $1/|\mathbf{p}|^2$ for $|\mathbf{p}| \to \infty$, the following relation holds for any real number $A > 0$:

$$\int d^3p \, \frac{\psi(\mathbf{p})\, e^{i\mathbf{p}\mathbf{L}}}{A - \mathbf{p}^2 + i\epsilon} \xrightarrow{|\mathbf{L}|\to\infty} -\frac{2\pi^2}{L}\psi(\sqrt{A}\tfrac{\mathbf{L}}{L})e^{i\sqrt{A}L} + \mathcal{O}(L^{-\frac{3}{2}})\,. \tag{9}$$

Effectively, this formula gives the form of the Feynman propagator for propagation over macroscopic distances. The parameter A corresponds to squared modulus of the on-shell momentum component of the propagating particle. Applying the Grimus-Stockinger theorem to our expression for $\mathcal{A}$, we find

$$\begin{aligned} i\mathcal{A} = \frac{-i}{8\pi^2 L}\mathcal{N}\sum_j \mathcal{M}_S^{\mu}\mathcal{M}_D^{\nu *}|U_{ej}|^2 \int_{-\infty}^{\infty} dt_1\, dt_2\, f_{\mathrm{H},S}(t_1)\, f^*_{\mathrm{He},S}(t_1)\, f_{\mathrm{He},D}(t_2)\, f^*_{\mathrm{H},D}(t_2) \\ \cdot \int_{-\infty}^{\infty} dp_0 \, \exp\left[-\frac{p_0^2 - m_j^2}{2\sigma_p^2}\right] e^{i\sqrt{p_0^2-m_j^2}L} e^{-i(E_{S,0}-p_0)t_1 + i(E_{D,0}-p_0)t_2} \\ \cdot \bar{u}_{e,S}\gamma_\mu(1-\gamma^5)(\not{p}_j + m_j)(1+\gamma^5)\gamma_\nu u_{e,D}\,, \end{aligned} \tag{10}$$

with $p_j \equiv (p_0, \sqrt{p_0^2 - m_j^2}\,\mathbf{L}/L)$ and with the constant

$$\begin{aligned} \mathcal{N} = \left(\frac{m_{\mathrm{H}}\omega_{\mathrm{H},S}}{\pi}\right)^{\frac{3}{4}} \left(\frac{m_{\mathrm{He}}\omega_{\mathrm{He},S}}{\pi}\right)^{\frac{3}{4}} \left(\frac{m_{\mathrm{He}}\omega_{\mathrm{He},D}}{\pi}\right)^{\frac{3}{4}} \left(\frac{m_{\mathrm{H}}\omega_{\mathrm{H},D}}{\pi}\right)^{\frac{3}{4}} \\ \cdot \left(\frac{2\pi}{m_{\mathrm{H}}\omega_{\mathrm{H},S} + m_{\mathrm{He}}\omega_{\mathrm{He},S}}\right)^{\frac{3}{2}} \left(\frac{2\pi}{m_{\mathrm{H}}\omega_{\mathrm{H},D} + m_{\mathrm{He}}\omega_{\mathrm{He},D}}\right)^{\frac{3}{2}} \end{aligned} \tag{11}$$

containing the wavefunction normalization factors from eq. (1) and the numerical prefactors that have arisen in the $\mathbf{x}_1$ and $\mathbf{x}_2$ integrations. Since we do not know the exact form of the modulation factors $f_{A,B}(t)$, we cannot evaluate the time integrals at this stage. However, ultimately, we are only interested in the transition rate Γ, which is proportional to $\langle \mathcal{A}\mathcal{A}^* \rangle$, the statistical average of $\mathcal{A}\mathcal{A}^*$ over all possible ^{3}H and ^{3}He states in the source and the detector. This expression can be simplified using statistical arguments. In particular, when evaluating it, we encounter the quantity

$$B_S(t_1, \tilde{t}_1) \equiv \left\langle f_{\mathrm{H},S}(t_1)\, f^*_{\mathrm{He},S}(t_1)\, f^*_{\mathrm{H},S}(\tilde{t}_1)\, f_{\mathrm{He},S}(\tilde{t}_1) \right\rangle = \left\langle \exp\left[-i \int_{\tilde{t}_1}^{t_1} dt'\, \Delta E_S(t') \right] \right\rangle, \tag{12}$$

and a similar term from the detector-related modulation factors. Here, t_1 and $\tilde{t}_1$ are the time variables appearing in the expressions for $\mathcal{A}$ and $\mathcal{A}^*$, respectively. To shorten the notation, we have defined a quantity $\Delta E_S(t') \equiv E_S(t') - E_{S,0} \equiv [E_{\mathrm{H},S}(t') - E_{\mathrm{He},S}(t')] - [E_{\mathrm{H},S,0} - E_{\mathrm{He},S,0}]$,

which gives the deviation of the energy of the neutrino emission line from its mean value at time t'. Following [23], we assume $\Delta E_S(t')$ to be a Gaussian random variable centered around zero:

$$\langle \Delta E_S(t') \rangle = 0\,. \tag{13}$$

Moreover, we assume fluctuations at different points in time to be uncorrelated (Markovian approximation), which implies

$$\Big\langle \Delta E_S(t')\, \Delta E_S(t'') \Big\rangle = \gamma_S\, \delta(t'-t'')\,. \tag{14}$$

This is a good approximation if the correlation time of the fluctuations is much smaller than all other time scales appearing in the problem, in particular the tritium life time and the running time of the experiment. The constant γ_S will turn out to be the width of the neutrino emission line. Proceeding along the lines of refs. [23, 30], we expand (12) into a Taylor series and obtain

$$B_S(t_1,\tilde{t}_1) = \sum_{n=0}^{\infty} \frac{(-i)^n}{n!} \int_{\tilde{t}_1}^{t_1} dt^{(1)} \cdots dt^{(n)} \left\langle\, \Delta E_S(t^{(1)}) \cdots \Delta E_S(t^{(n)}) \right\rangle\,. \tag{15}$$

One can now use the assumption that $\Delta E_S(t^{(i)})$ is normally distributed around zero to show that the n-point correlation functions on the right hand side can, for even n, be rewritten by splitting them into products of two-point functions (which can be evaluated by using (14)) and summing over all $(n-1)(n-3)\cdots 3\cdot 1 = n!/[2^{n/2}(n/2)!]$ distinct combinations of such two-point functions. For odd n, the n-point correlation functions can be transformed into products of $(n-1)/2$ two-point functions and a one-point function, which is zero by virtue of eq. (13). Therefore, $B_S(t_1,\tilde{t}_1)$ takes the form

$$\begin{aligned} B_S(t_1,\tilde{t}_1) &= \sum_{n=0}^{\infty} \frac{(-\gamma_S/2)^n}{n!} \prod_{i=1}^{n} \int_{\tilde{t}_1}^{t_1} dt^{(2i)}\, dt^{(2i-1)}\, \delta(t^{(2i)} - t^{(2i-1)}) \\ &= \exp\Big[-\frac{1}{2}\gamma_S |t_1 - \tilde{t}_1| \Big]\,. \end{aligned} \tag{16}$$

The analogous expression for the detector-related modulation factors is

$$B_D(t_2,\tilde{t}_2) = \exp\Big[-\frac{1}{2}\gamma_D |t_2 - \tilde{t}_2| \Big]\,. \tag{17}$$

Using

$$\begin{aligned} \int_{-\infty}^{\infty} dt_1\, d\tilde{t}_1\, dt_2\, d\tilde{t}_2 \exp\Big[-\frac{1}{2}\gamma_S |t_1-\tilde{t}_1| - i(E_{S,0}-p_0)t_1 + (E_{S,0}-\tilde{p}_0)t_1 \Big] \\ \cdot \exp\Big[-\frac{1}{2}\gamma_D |t_2-\tilde{t}_2| + i(E_{D,0}-p_0)t_2 - (E_{D,0}-\tilde{p}_0)t_2 \Big] \\ = (2\pi)^4 [\delta(p_0-\tilde{p}_0)]^2 \frac{\gamma_S/2\pi}{(E_{S,0}-p_0)^2 + \gamma_S^2/4} \frac{\gamma_D/2\pi}{(E_{D,0}-p_0)^2 + \gamma_D^2/4}\,, \end{aligned} \tag{18}$$

the expression for $\langle \mathcal{A}\mathcal{A}^* \rangle$ now becomes

$$\begin{aligned}\langle \mathcal{A}\mathcal{A}^* \rangle = \frac{\mathcal{N}^2}{64\pi^4 L^2} \sum_{j,k} \mathcal{M}_S^{\mu} \mathcal{M}_D^{\nu *} \mathcal{M}_S^{\rho *} \mathcal{M}_D^{\sigma} |U_{ej}|^2 |U_{ek}|^2 \int_{-\infty}^{\infty} dp_0 \, d\tilde{p}_0 \exp\left[- \frac{2p_0^2 - m_j^2 - m_k^2}{2\sigma_p^2} \right] \\ \cdot (2\pi)^4 [\delta(p_0 - \tilde{p}_0)]^2 \frac{\gamma_S/2\pi}{(E_{S,0} - p_0)^2 + \gamma_S^2/4} \frac{\gamma_D/2\pi}{(E_{D,0} - p_0)^2 + \gamma_D^2/4} e^{i\left(\sqrt{p_0^2 - m_j^2} - \sqrt{p_0^2 - m_k^2}\right) L} \\ \cdot \bar{u}_{e,S} \gamma_\mu (1 - \gamma^5)(\not{p}_j + m_j)(1 + \gamma^5) \gamma_\nu u_{e,D} \bar{u}_{e,D} \gamma_\sigma (1 - \gamma^5)(\not{\tilde{p}}_j + m_k)(1 + \gamma^5) \gamma_\rho u_{e,D} \, .\end{aligned} \tag{19}$$

We can rewrite the squared δ-function as $T/2\pi \cdot \delta(p_0 - \tilde{p}_0)$ (with T the total running time of the experiment), and use the remaining δ-factor to evaluate the $\tilde{p}_0$ integral. We are left with the p_0 integration, which receives its main contribution from the region where $|E_{S,0} - p_0| \lesssim \gamma_S$ and $|E_{D,0} - p_0| \lesssim \gamma_D$ due to the Lorentzians on the right hand side of eq. (19). Since $\gamma_{S,D} \ll \sigma_p$ and $\gamma_{S,D} \ll E_{S,0}, E_{D,0}$, the spinorial factors as well as the real exponential that will lead to the generalized Lamb-Mössbauer factor and to the localization term are almost constant over this region and may be replaced by their values at

$$\bar{E} = \frac{1}{2}(E_{S,0} + E_{D,0}) \, . \tag{20}$$

If we finally expand the oscillation phase in $\Delta m_{jk}^2 / p_0^2$, the p_0 integral becomes [1]

$$\begin{aligned} I_{jk} &\equiv \int_{-\infty}^{\infty} dp^0 \, \frac{\gamma_S/2\pi}{(p^0 - E_{S,0})^2 + \gamma_S^2/4} \, \frac{\gamma_D/2\pi}{(p^0 - E_{D,0})^2 + \gamma_D^2/4} \, \exp\left[- i \frac{\Delta m_{jk}^2 L}{2p^0} \right] \\ &= \frac{1}{2\pi} \frac{1}{(E_{S,0} - E_{D,0})^2 + \frac{(\gamma_S + \gamma_D)^2}{4}} \left\{ \frac{\gamma_S + \gamma_D}{2} (A_{jk}^{(S)} + A_{jk}^{(D)}) \right. \\ &\qquad \left. - \frac{1}{2} \frac{(A_{jk}^{(S)} - A_{jk}^{(D)}) \left[(E_{S,0} - E_{D,0})(\gamma_S - \gamma_D) \pm i \frac{(\gamma_S + \gamma_D)^2}{2} \right]}{E_{S,0} - E_{D,0} \pm i \, \frac{\gamma_S - \gamma_D}{2}} \right\} , \end{aligned} \tag{21}$$

with the abbreviations

$$\begin{aligned} A_{jk}^{(B)} &= \exp\left[- i \frac{\Delta m_{jk}^2}{2(E_{B,0} \pm i \, \frac{\gamma_B}{2})} \, L \right] \\ &\simeq \exp\left[- 2\pi i \frac{L}{L_{B,jk}^{\mathrm{osc}}} \right] \exp\left[- \frac{L}{L_{B,jk}^{\mathrm{coh}}} \right] , \end{aligned} \tag{22}$$

and with the oscillation and coherence lengths

$$L_{B,jk}^{\mathrm{osc}} = \frac{4\pi E_{B,0}}{\Delta m_{jk}^2} \simeq \frac{4\pi \bar{E}}{\Delta m_{jk}^2} \qquad \text{and} \qquad L_{B,jk}^{\mathrm{coh}} = \frac{4E_{B,0}^2}{\gamma_B |\Delta m_{jk}^2|} \simeq \frac{4\bar{E}^2}{\gamma_B |\Delta m_{jk}^2|} \, . \tag{23}$$

In eq. (21), the upper (lower) signs correspond to $\Delta m_{jk}^2 > 0$ ($\Delta m_{jk}^2 < 0$). Thus, the transition rate Γ for a Mössbauer neutrino experiment dominated by homogeneous line

broadening is, according to Fermi's Golden Rule,

$$\Gamma = \frac{\Gamma_0\, B_0}{4\pi L^2}\, Y_S Y_D\, \frac{1}{2\pi} \sum_{j,k} |U_{ej}|^2 |U_{ek}|^2 \exp\left[-\frac{2\bar{E}^2 - m_j^2 - m_k^2}{2\sigma_p^2} \right] \frac{1}{(E_{S,0} - E_{D,0})^2 + \frac{(\gamma_S+\gamma_D)^2}{4}}$$
$$\cdot \left[\frac{\gamma_S + \gamma_D}{2}(A_{jk}^{(S)} + A_{jk}^{(D)}) - \frac{1}{2} \frac{(A_{jk}^{(S)} - A_{jk}^{(D)}) \left[(E_{S,0} - E_{D,0})(\gamma_S - \gamma_D) \pm i \frac{(\gamma_S+\gamma_D)^2}{2} \right]}{E_{S,0} - E_{D,0} \pm i\, \frac{\gamma_S - \gamma_D}{2}} \right], \quad (24)$$

where

$$\Gamma_0 \equiv \frac{G_F^2 \cos^2\theta_c}{\pi}\, |\psi_e(R)|^2\, m_e^2 \left(|M_V|^2 + g_A^2 |M_A|^2 \right) \left(\frac{E_{S,0}}{m_e} \right)^2 \kappa_S \quad (25)$$

is the rate of bound state ^{3}H decay, and

$$B_0 \equiv 4\pi G_F^2 \cos^2\theta_c\, |\psi_e(R)|^2 \left(|M_V|^2 + g_A^2 |M_A|^2 \right) \kappa_D \quad (26)$$

is related to the cross section for induced orbital electron capture on *free* ^{3}He by [31]

$$\sigma(E_\nu) = B_0\, \rho(E_{\bar{\nu},\mathrm{res}})\,. \quad (27)$$

Here $\rho(E_{\bar{\nu},\mathrm{res}})$ is the spectral density of incident neutrinos, i.e. the number of neutrinos per unit energy interval, at the resonance energy for this case, $E_{\bar{\nu},\mathrm{res}} = Q + E_R$ (where $Q = 18.6$ keV is the Q-value of the process and E_R is the recoil energy transferred to the atom). The quantities Y_S and Y_D in eq. (24) are given by

$$Y_B = 8 \left(\sqrt{\frac{m_{\mathrm{H}}\, \omega_{\mathrm{H},B}}{m_{\mathrm{He}}\, \omega_{\mathrm{He},B}}} + \sqrt{\frac{m_{\mathrm{He}}\, \omega_{\mathrm{He},B}}{m_{\mathrm{H}}\, \omega_{\mathrm{H},B}}} \right)^{-3} \quad (28)$$

for $B = \{S, D\}$.

As anticipated, (24) coincides precisely with the corresponding expression for the case of inhomogeneous line broadening, given in eq. (41) of ref. [1].[2] We find again a Breit-Wigner-like resonance term, which suppresses Mössbauer transitions if the central energies $E_{S,0}$ and $E_{D,0}$ of the emission and absorption lines differ by more than the average line width $(\gamma_S + \gamma_D)/2$, and a factor

$$\exp\left[-\frac{2\bar{E}^2 - m_j^2 - m_k^2}{2\sigma_p^2} \right] = \exp\left[-\frac{(p_{jk}^{\min})^2}{\sigma_p^2} \right] \exp\left[-\frac{|\Delta m_{jk}^2|}{2\sigma_p^2} \right], \quad (29)$$

with

$$(p_{jk}^{\min})^2 = \bar{E}^2 - \max(m_j^2, m_k^2)\,, \quad (30)$$

which we interpret as a generalized Lamb-Mössbauer factor (or fraction of recoil-free emissions/absorptions), multiplied with a localization term. The latter can be neglected if $\sigma_p^2 \gg$

[2] In the present work, we have chosen to present Γ in a form where the Breit-Wigner term is factorized out of the term containing the oscillation and coherence exponentials. It is straightforward to check that this form is identical to the form used in ref. [1].

Δm^2_{jk}, or equivalently, if $L^{\rm osc}_{B,jk} \gg 4\pi\sigma_x\bar{E}/\sigma_p$, where $\sigma_x \equiv 1/2\sigma_p$ is the spatial delocalization of the emitting and absorbing atoms. For $\bar{E} = 18.6$ keV and $\sigma_p \sim (m_H\theta_D)^{1/2} \sim 7$ keV, it is clear that this inequality is easily fulfilled since σ_x is of the order of the interatomic distance, while $L^{\rm osc}_{B,jk} \sim 20$ m for oscillations driven by the atmospheric mass squared difference Δm^2_{31} and $L^{\rm osc}_{B,jk} \sim 600$ m for oscillations driven by the solar mass squared difference Δm^2_{21}. The factors $A^{(B)}_{jk}$ in eq. (24) contain the oscillation exponentials and the decoherence terms which describe the effect of wave packet separation due to the different group velocities associated with different neutrino mass eigenstates. However, it is easy to see that decoherence is not an issue in any realistic Mössbauer neutrino experiment because the corresponding coherence lengths are of $\mathcal{O}(10^{13}$ km).

The fact that the formula for Γ is identical for the cases of homogeneous and inhomogeneous line broadening implies that these two situations cannot be distinguished experimentally. This confirms a more general theorem by Kiers, Nussinov, and Weiss [32] which states that it is impossible to distinguish an ensemble of neutrino wave packets with identical momentum distributions from an ensemble of plane wave neutrinos whose individual momenta follow the same distribution. In fact, the density matrix describing the ensemble is identical for both cases. Applied to Mössbauer neutrinos, the case of neutrino wave packets corresponds to a situation where homogeneous line broadening is dominant, so that each neutrino wave packet is broadened because the energy of the emission line, E_S, changes during the emission process. In contrast, for mostly inhomogeneous line broadening, each individual neutrino can be approximately described by a plane wave because it is emitted with an extremely small energy spread (which is ultimately determined by subdominant homogeneous solid state effects, by the natural width, and by the Heisenberg principle). Different neutrinos, however, are emitted with different energies which depend, for example, on the proximity of the emitting atom to crystal impurities and lattice defects.

To end this section, let us give a simpler and more useful form of eq. (24), obtained by neglecting the localization and coherence terms and considering the two-flavor approximation, with an effective mixing angle θ, an effective mass squared difference Δm^2, and an average absolute neutrino mass $\bar{m}$ [1]:

$$\Gamma \simeq \frac{\Gamma_0\, B_0}{4\pi L^2}\, Y_S Y_D\, \exp\left[-\frac{\bar{E}^2-\bar{m}^2}{\sigma_p^2}\right] \frac{(\gamma_S+\gamma_D)/2\pi}{(E_{S,0}-E_{D,0})^2+\frac{(\gamma_S+\gamma_D)^2}{4}} \left\{1-\sin^2 2\theta\, \sin^2\left(\pi\frac{L}{L^{\rm osc}}\right)\right\}. \tag{31}$$

3 Mössbauer neutrinos in quantum mechanics: Lorentzian wave packets

Let us now discuss how oscillations of Mössbauer neutrinos can be understood in the framework of quantum mechanics. Since QM is unable to describe particle creation and destruction, we cannot directly include the production and detection processes into our formalism, as in QFT. Instead, we will first compute the probability for transitions between the initial and final neutrino states, and then multiply this with the emitted flux and with the absorption cross section to obtain the overall event rate Γ. We will describe the propagating neutrino as a superposition of three wave packets, one for each mass eigenstate [32, 33, 34, 35, 36, 37]. As we have discussed above, such a description corresponds

to Mössbauer neutrinos in the regime of homogeneous line broadening, while the case of inhomogeneous broadening would be more naturally implemented by considering an ensemble of many plane wave neutrinos in the density matrix approach [32]. However, since homogeneous and inhomogeneous line broadening cannot be distinguished experimentally, it is sufficient to focus on one of the two cases. We use the wave packet picture because it provides insights into the evolution of each single neutrino, which we find useful to better understand the localization and coherence conditions that will emerge.

Unlike most other authors, who use wave packets with a Gaussian shape, we will use wave packets with a Lorentzian momentum distribution because it is known from the classical Mössbauer effect that homogeneous and inhomogeneous line broadening mechanisms lead to a Lorentzian energy spread [38, 39]. The momentum space wave function for the electron antineutrino produced in ^{3}H decay thus has the form

$$\langle p|\bar{\nu}_{eS}(t)\rangle = \frac{1}{N_S}\sum_j U_{ej}\, f_{jS}\, \frac{\sqrt{\gamma_S/2\pi}}{p - p_{jS} + i\gamma_S/2}\, \exp\big[-iE_j t\big]\, |\nu_j\rangle\,. \tag{32}$$

The index S indicates that this state is produced in the neutrino source, and the normalization factor is $N_S = \big(\sum_j |U_{ej}|^2\, |f_{jS}|^2\big)^{1/2}$. Similarly, the detection process can be described as a projection of $|\bar{\nu}_{eS}(t)\rangle$ onto a state $|\bar{\nu}_{eD}\rangle$ with the momentum space representation

$$\langle p|\bar{\nu}_{eD}\rangle = \frac{1}{N_D}\sum_j U_{ej}\, f_{jD}\, \frac{\sqrt{\gamma_D/2\pi}}{p - p_{jD} + i\gamma_D/2}\, \exp\big[-ipL\big]\, |\nu_j\rangle \tag{33}$$

and the normalization factor $N_D = \big(\sum_j |U_{ej}|^2\, |f_{jS}|^2\big)^{1/2}$. In the above expressions, p_{jS}, p_{jD} are the central momenta of the wave packets, $E_j = (p^2 + m_j^2)^{1/2}$, and γ_S, γ_D are the wave packet widths. Moreover, we have introduced phenomenological fudge factors f_{jS}, f_{jD} that will be motivated and discussed below.

For Mössbauer neutrinos, γ_S and γ_D are of the order of the energy uncertainty associated with the emission and detection processes, which is of order 10^{-11} eV. The much larger *momentum* uncertainties of the source and the detector do not play a role because the neutrino is on-shell, so that by virtue of the relativistic energy-momentum relation the momentum uncertainty of the neutrino cannot be larger than its energy uncertainty. (Of course, the momenta associated with the different mass eigenstates have to differ by much more than 10^{-11} eV in order to ensure energy-momentum conservation in the production and detection processes.)

Note that $|\bar{\nu}_{eD}\rangle$ is time-independent (on this point, we disagree with ref. [37], where the detection operator $|\nu_{\beta D}\rangle\langle\nu_{\beta D}|$ is assumed to be not a time-independent but only a time-averaged quantity); on the other hand, a factor $\exp[-ipL]$ is required to center the wave packet around $x = L$.

The phenomenological fudge factors f_{jS} and f_{jD} can be used to describe a possible mass dependence of the neutrino production and detection amplitudes. For example, we have seen in the previous section that the Lamb-Mössbauer factor depends on m_j, so that the production and absorption of the lighter neutrino mass eigenstates is slightly suppressed compared to the production and absorption of the heavier ones. This can be viewed as a

slight dynamical reduction of neutrino mixing. Let us stress that f_{jS} and f_{jD} cannot be determined in the QM approach, and have to be put in by hand. We will choose

$$f_{jS} \equiv \exp\left[\frac{\bar{E}^2 - m_j^2}{2\sigma_{pS}^2}\right], \qquad f_{jD} \equiv \exp\left[\frac{\bar{E}^2 - m_j^2}{2\sigma_{pD}^2}\right] \tag{34}$$

(with σ_{pS}, σ_{pD}, and $\bar{E}$ defined as in eqs. (7) and (20), respectively) in order to ultimately reproduce the correct Lamb-Mössbauer factor.

The amplitude for the transition $|\bar{\nu}_{eS}(t)\rangle \to |\bar{\nu}_{eD}\rangle$ is given by

$$\mathcal{A}(t,L) = \langle \bar{\nu}_{eD} | \bar{\nu}_{eS}(t)\rangle = \int dp\ \langle \bar{\nu}_{eD}|p\rangle\, \langle p|\bar{\nu}_{eS}(t)\rangle\ . \tag{35}$$

To be able to evaluate this integral, we make use of the smallness of γ_S and γ_D, and expand E_j around the average momentum $\bar{p}_j = (p_{jS} + p_{jD})/2$, which gives

$$E_j = \sqrt{p^2 + m_j^2}\ t \simeq \bar{E}_j\, t + \bar{v}_j t(p - \bar{p}_j)\,, \tag{36}$$

with the definitions

$$\bar{E}_j = \sqrt{\bar{p}_j^2 + m_j^2} \qquad \text{and} \qquad \bar{v}_j = \frac{\bar{p}_j}{\sqrt{\bar{p}_j^2 + m_j^2}}\,. \tag{37}$$

This approximation corresponds to neglecting dispersion (wave packet spreading), which is a second-order effect [40]. Eq. (36) is a good approximation as long as $(p - \bar{p}_j)/\bar{E}_j \ll \bar{E}_j^2/m_j^2$ for all p within the peak regions of the source and detector wave packets. We can now compute $\mathcal{A}(t,L)$, and obtain

$$\begin{aligned}\mathcal{A}(t,L) = {} & \frac{1}{N_S N_D} \sum_j |U_{ej}|^2\, f_{jS} f_{jD}^*\, \frac{-i\gamma_S}{p_{jS} - p_{jD} - i(\gamma_S + \gamma_D)/2} \exp\big[-i\bar{E}_j t + i\bar{v}_j \bar{p}_j t\big] \\ & \cdot \left\{ \exp\left[\left(ip_{jS} + \frac{\gamma_S}{2}\right)(L - \bar{v}_j t)\right]\theta(\bar{v}_j t - L) + \exp\left[\left(ip_{jD} - \frac{\gamma_D}{2}\right)(L - \bar{v}_j t)\right]\theta(-\bar{v}_j t + L)\right\},\end{aligned} \tag{38}$$

where θ denotes the Heaviside step function.

The next step is to compute the transition probability for the process $|\bar{\nu}_{eS}\rangle \to |\bar{\nu}_{eD}\rangle$, defined by

$$\mathcal{P}(L) = \frac{1}{T}\int_{-T/2}^{T/2} dt\, \mathcal{A}^*(t,L)\, \mathcal{A}(t,L)\,. \tag{39}$$

Here, the incoherent averaging over the running time T of the experiment reflects the fact that we do not precisely know at which point in time the production and detection reactions take place. (The detection time is, of course, implicitly constrained by the fact that the neutrino wave packet has sizeable overlap with the detector only during a very short time interval.) Physically, $\mathcal{P}(L)$ gives the time-averaged probability that a neutrino prepared in the state $|\bar{\nu}_{eS}(0)\rangle$ at $t = 0$ is detected as $|\bar{\nu}_{eD}\rangle$ at a later time. Note that $\mathcal{P}(L)$ is

not a $\bar{\nu}_e$ survival probability in the usual sense because in general $\mathcal{P}(L)\,|_{\Delta m^2_{jk}=0} \neq 1$. In particular, irrespective of the neutrino mixing parameters, $\mathcal{P}(L)$ can only be sizeable if the wave packets $|\bar{\nu}_{eS}(t)\rangle$ and $|\bar{\nu}_{eD}\rangle$ have sufficient overlap in momentum space. This is precisely the Mössbauer resonance condition.

The experimentally observable event rate Γ is obtained by multiplying $\mathcal{P}(L)$ with the Mössbauer neutrino emission rate $\Gamma_0^{\rm MB}$, the Mössbauer neutrino detection cross section $\sigma^{\rm MB}$, and the geometrical flux suppression factor $1/4\pi L^2$:

$$\Gamma = \frac{1}{4\pi L^2}\,\Gamma_0^{\rm MB}\,\mathcal{P}(L)\,\sigma^{\rm MB} \tag{40}$$

$$\equiv \frac{1}{4\pi L^2}\Big(\Gamma_0\,Y_S\,\sum_j |U_{ej}|^2|f_{jS}|^2\Big)\,\mathcal{P}(L)\,\Big(B_0 Y_D \frac{T}{2\pi}\,\sum_j |U_{ej}|^2|f_{jD}|^2\Big)\,. \tag{41}$$

The parenthesized expressions for $\Gamma_0^{\rm MB}$ and $\sigma^{\rm MB}$ have to be derived in the QFT formalism discussed in sec. 2 and ref. [1]. It is impossible to derive them in QM because they describe particle creation and annihilation processes. Note that we are here using the cross section for the limiting case of an infinitely sharp Mössbauer resonance — hence the factor $T/2\pi$, which should be understood as an approximate δ-peak of the form

$$\delta(0) \simeq \lim_{E\to E_{D,0}} \int_{-T/2}^{T/2} dt\, e^{i(E-E_{D,0})t} = \frac{T}{2\pi}\,. \tag{42}$$

The effect of line broadening is already accounted for by the fact that $\mathcal{A}(t,L)$ is suppressed if $|p_{jS}-p_{jD}| \gg (\gamma_S+\gamma_D)/2$ (cf. eq. (38)).

Evaluation of Γ requires splitting the time integral in eq. (39) into three separate integrals with integration domains $(-\infty, L/\bar{v}_k]$, $(L/\bar{v}_k, L/\bar{v}_j)$, $[L/\bar{v}_j, \infty)$ for $m_j > m_k$, and $(-\infty, L/\bar{v}_j]$, $[L/\bar{v}_j, L/\bar{v}_k]$, $[L/\bar{v}_k, \infty)$ for $m_j < m_k$. (It is justified to replace the integration boundaries $\pm T/2$ from eq. (39) by infinity here because the overlap of the wave packets $|\bar{\nu}_{eS}(t)\rangle$ and $|\bar{\nu}_{eD}\rangle$ decreases exponentially at large T, when the neutrino has long passed the detector.) We will only show how to evaluate one of the above integrals, since the others are similar. Consider

$$J_{jk} = \int_{L/\bar{v}_k}^{L/\bar{v}_j} dt\, \exp\Big[-i(\bar{E}_j - \bar{E}_k)t + i(\bar{v}_j\bar{p}_j - \bar{v}_k\bar{p}_k)t - i(\bar{v}_j p_{jD} - \bar{v}_k p_{kS})t$$
$$+ \frac{1}{2}(\gamma_D\bar{v}_j - \gamma_S\bar{v}_k)t + i(p_{jD}-p_{kS})L - \frac{1}{2}(\gamma_D-\gamma_S)L\Big] \tag{43}$$

for $m_j > m_k$. We use the approximation of ultrarelativistic neutrinos ($m_j \ll \bar{E}_j$), which suggests the expansions

$$p_{jS} \simeq E_{S,0} - (1-\xi_S)\frac{m_j^2}{2E_{S,0}}\,, \qquad p_{jD} \simeq E_{D,0} - (1-\xi_D)\frac{m_j^2}{2E_{D,0}}\,, \tag{44}$$

from which it follows that

$$\bar{E}_j \simeq \bar{E} + \bar{\xi}\frac{m_j^2}{2\bar{E}}\,, \qquad \bar{p}_j \simeq \bar{E} - (1-\bar{\xi})\frac{m_j^2}{\bar{E}}\,, \qquad \bar{v}_j \simeq 1 - \frac{m_j^2}{2\bar{E}^2}\,, \tag{45}$$

where

$$\bar{E} \equiv \frac{1}{2}(E_{S,0} + E_{D,0}) \qquad \text{and} \qquad 1 - \bar{\xi} \equiv \frac{\bar{E}}{2}\left(\frac{1-\xi_S}{E_{S,0}} + \frac{1-\xi_D}{E_{D,0}}\right). \tag{46}$$

In these expressions, $E_{S,0}$ and $E_{D,0}$ are the mean energies for the case of massless neutrinos, and ξ_S, ξ_D are constant parameters determined by the properties of the source and the detector, respectively. These parameters can be calculated only in an explicit treatment of the neutrino production and detection processes. For conventional neutrino sources, ξ_S and ξ_D are of $\mathcal{O}(1)$, but for Mössbauer neutrinos, the energies associated with different neutrino mass eigenstates have to coincide within the line widths γ_S and γ_D, so that ξ_S, ξ_D and $\bar{\xi}$ must be extremely small in this case. Indeed, we will see below that, in order to reproduce our QFT result (24), we have to take $\xi_S = \xi_D = 0$.

Plugging (45) into (43), neglecting terms containing the small product $\Delta m^2_{jk}(E_{S,0} - E_{D,0})/\bar{E}^2$ and, in the denominator, also neglecting terms of order $\tilde{\gamma} m_j^2/\bar{E}^2$, we obtain

$$J_{jk} = \frac{A^{(S)}_{jk} - A^{(D)}_{jk}}{\frac{1}{2}(\gamma_D - \gamma_S) + i(E_{S,0} - E_{D,0}) - i\bar{\xi}\Delta m^2_{jk}/2\bar{E}} \tag{47}$$

with the oscillation and coherence terms abbreviated as

$$\begin{aligned} A^{(B)}_{jk} &= \exp\left[-i\frac{\Delta m^2_{jk} L}{2\bar{E}} - \frac{|\Delta m^2_{jk}|\gamma_B L}{4\bar{E}^2}\right] \\ &\equiv \exp\left[-2\pi i \frac{L}{L^{\text{osc}}_{jk}} - \frac{L}{L^{\text{coh}}_{B,jk}}\right]. \end{aligned} \tag{48}$$

for $B = \{S, D\}$. Note that the $A^{(B)}_{jk}$ are identical to the quantities of the same name defined in eq. (22), up to the replacement of $E_{B,0}$ by $\bar{E}$, which leads to corrections of $\mathcal{O}(\Delta m^2_{jk}(E_{S,0} - E_{D,0})/\bar{E}^2)$. Since we have neglected terms of this order in the derivation of (47), we should for consistency also neglect them here. The full expression for Γ is

$$\begin{aligned} \Gamma = {} & \frac{\Gamma_0 B_0}{4\pi L^2} Y_S Y_D \frac{1}{2\pi} \sum_{j,k} |U_{ej}|^2 |U_{ek}|^2 \exp\left[-\frac{2\bar{E}^2 - m_j^2 - m_k^2}{2\sigma_p^2}\right] \gamma_S \gamma_D \\ & \cdot \left[E_{S,0} - E_{D,0} - m_j^2 \left(\frac{1-\xi_S}{2E_{S,0}} - \frac{1-\xi_D}{2E_{D,0}}\right) - \frac{i(\gamma_S + \gamma_D)}{2}\right]^{-1} \\ & \cdot \left[E_{S,0} - E_{D,0} - m_k^2 \left(\frac{1-\xi_S}{2E_{S,0}} - \frac{1-\xi_D}{2E_{D,0}}\right) + \frac{i(\gamma_S + \gamma_D)}{2}\right]^{-1} \\ & \cdot \left\{ \frac{A^{(S)}_{jk}}{\gamma_S + i\xi_S \frac{\Delta m^2_{jk}}{2E_{S,0}}} + \frac{A^{(D)}_{jk}}{\gamma_D - i\xi_D \frac{\Delta m^2_{jk}}{2E_{D,0}}} + \frac{A^{(S)}_{jk} - A^{(D)}_{jk}}{\frac{1}{2}(\gamma_D - \gamma_S) \pm i(E_{S,0} - E_{D,0}) - i\bar{\xi}\frac{\Delta m^2_{jk}}{2\bar{E}}} \right\}. \end{aligned} \tag{49}$$

In the last term, the upper sign applies to the case $\Delta m^2_{jk} > 0$, while the lower one is for $\Delta m^2_{jk} < 0$. As discussed above, ξ_S and ξ_D are very small for Mössbauer neutrinos. If we

neglect them completely, Γ simplifies to

$$\Gamma = \frac{\Gamma_0 B_0}{4\pi L^2}\, Y_S Y_D \frac{1}{2\pi} \sum_{j,k} |U_{ej}|^2 |U_{ek}|^2 \, \exp\left[- \frac{2\bar{E}^2 - m_j^2 - m_k^2}{2\sigma_p^2} \right] \frac{1}{(E_{S,0} - E_{D,0})^2 + \frac{1}{4}(\gamma_S + \gamma_D)^2}$$

$$\cdot \left[\frac{\gamma_S + \gamma_D}{2} (A_{jk}^{(S)} + A_{jk}^{(D)}) - \frac{1}{2} \frac{(A_{jk}^{(S)} - A_{jk}^{(D)}) \left[(E_{S,0} - E_{D,0})(\gamma_S - \gamma_D) \pm i \frac{(\gamma_S + \gamma_D)^2}{2} \right]}{E_{S,0} - E_{D,0} \pm i \frac{\gamma_S - \gamma_D}{2}} \right] . \quad (50)$$

This equation is identical to our QFT result, eq. (24) (within the approximations made in the two approaches). In particular, we find the same oscillation, coherence, and resonance terms.

4 Discussion and conclusions

Let us now summarize and discuss our results. In the first part of this paper, we have used quantum field theoretical techniques to derive the rate Γ of Mössbauer neutrino emission, propagation, and absorption (eq. (24)). For the first time, we have explicitly included the effect of homogeneous line broadening due to fluctuating electromagnetic fields in the solid state crystals forming the source and the detector. We have confirmed the expectation from ref. [1] that the resulting formula for Γ agrees precisely with the one obtained in [1] for the case of inhomogeneous line broadening caused by crystal defects and impurities. In particular, we have confirmed that, also for homogeneous line broadening, Γ has a Breit-Wigner-like resonance structure, and contains oscillation, localization, and coherence exponentials. Moreover, our formula accounts for the suppression of recoilless emission and absorption processes compared to their non-recoilless counterparts through a generalized Lamb-Mössbauer factor. We have also noted that in realistic experiments the localization and decoherence terms are irrelevant and may be set equal to unity. The localization term enforces the condition that the quantum mechanical delocalization of the neutrino source and detector have to be small compared to the oscillation lengths for oscillations to take place, a condition that is easily fulfilled in any oscillation experiment. The decoherence term, on the other hand, accounts for the possibility of wave packet separation due to the different group velocities associated with different neutrino mass eigenstates, but also this does not happen in terrestrial experiments.

We have then proceeded to a derivation of Γ in a quantum mechanical approach, in which the neutrino is described by a Lorentzian wave packet of the form (32). We have arrived at eq. (50), which coincides with the QFT result (24). However, since the neutrino production and detection processes, which involve particle creation and annihilation, cannot be described in QM, the Mössbauer neutrino production rate as well as the detection cross section had to be put in by hand. Also, the properties of the neutrino wave packets (shape, width, central momenta) had to be chosen in an ad hoc way instead of emerging naturally from the formalism or being related to properties of the source and the detector. Once the appropriate choices for these parameters are made, the Breit-Wigner-shaped resonance factor as well as the oscillation and decoherence terms can be derived. The correct Lamb-Mössbauer and localization factors are obtained only if suitably chosen phenomenological weighting factors f_{jS}, f_{jD} for the different neutrino mass eigenstates are introduced in the

neutrino wave function to account for the tiny dependence of the emission and absorption probabilities on the neutrino mass.

As expected, Γ factorizes into the emitted neutrino flux, a transition probability $\mathcal{P}(L)$, and the detection cross section. While in the QM approach, this property is introduced as an assumption in eq. (40), it emerges naturally in QFT. The reason is that for large propagation distance L off-shell effects become negligible, and according to the Grimus-Stockinger theorem eq. (9) the propagator then reduces to the exponential phase factor $\exp(ipL)$ (with p being the modulus of the neutrino momentum), which is also used in QM to describe the spatial evolution of particles.

In conclusion, we have shown that the QM approach to Mössbauer neutrino oscillations, in which the production, propagation, and detection processes are treated separately, is able to reproduce the results obtained in the QFT approach, in which these processes are a priori considered as a single entity and their factorization emerges as a result. In general, the framework of QFT is significantly more robust because it does not require any assumptions on the neutrino wave function, whose parameters are instead automatically determined from the much less ambiguous properties of the neutrino source and the detector. For example, homogeneous and inhomogeneous line broadening are easy to implement in QFT (see sec. 2 and ref. [1]), while in QM, they have to be accounted for by choosing appropriate wave packet widths. Also, the emission rate, the detection cross section, and the Lamb-Mössbauer factor cannot be predicted in QM and have to be put in by hand. On the other hand, the QM approach can give a better physical understanding of the origin of oscillation, decoherence, and resonance phenomena once all free parameters are chosen appropriately, e.g. by matching with the QFT result.

Acknowledgments

It is a pleasure to thank Evgeny Akhmedov, Samoil Bilenky, Franz von Feilitzsch, Manfred Lindner, and Walter Potzel for interesting and helpful discussions. This work was in part supported by the Transregio Sonderforschungsbereich TR27 "Neutrinos and Beyond" der Deutschen Forschungsgemeinschaft. The author would also like to acknowledge support from the Studienstiftung des Deutschen Volkes.

---

[1] E. K. Akhmedov, J. Kopp, and M. Lindner, JHEP **05**, 005 (2008), 0802.2513.
[2] W. M. Visscher, Phys. Rev. **116**(6), 1581 (1959).
[3] W. P. Kells, AIP Conf. Proc. **99**, 272 (1983).
[4] W. P. Kells and J. P. Schiffer, Phys. Rev. **C28**, 2162 (1983).
[5] R. S. Raghavan (2005), hep-ph/0511191.
[6] R. S. Raghavan (2006), hep-ph/0601079.
[7] W. Potzel, Phys. Scripta **T127**, 85 (2006).
[8] W. Potzel, J. Phys. Conf. Ser. **136**, 022010 (2008), 0810.2170.
[9] H. Minakata and S. Uchinami, New J. Phys. **8**, 143 (2006), hep-ph/0602046.
[10] S. M. Bilenky, F. von Feilitzsch, and W. Potzel, J. Phys. **G34**, 987 (2007), hep-ph/0611285.

[11] S. M. Bilenky (2007), arXiv:0708.0260[hep-ph].
[12] S. M. Bilenky, F. von Feilitzsch, and W. Potzel, J. Phys. **G35**, 095003 (2008), 0803.0527.
[13] E. K. Akhmedov, J. Kopp, and M. Lindner (2008), 0803.1424.
[14] S. M. Bilenky, F. von Feilitzsch, and W. Potzel (2008), 0804.3409.
[15] S. J. Parke, H. Minakata, H. Nunokawa, and R. Z. Funchal, Nucl. Phys. Proc. Suppl. **188**, 115 (2009), 0812.1879.
[16] A. G. Cohen, S. L. Glashow, and Z. Ligeti (2008), 0810.4602.
[17] R. S. Raghavan (2008), 0806.0839.
[18] R. S. Raghavan (2008), 0805.4155.
[19] R. S. Raghavan, Phys. Rev. Lett. **102**, 091804 (2009), 0903.0787.
[20] W. Potzel and F. E. Wagner (2009), paper submitted to PRL.
[21] R. Coussement, G. S'heeren, M. Van Den Bergh, and P. Boolchand, Phys. Rev. B **45**(17), 9755 (1992).
[22] H. J. Lipkin, *Quantum mechanics: New approaches to selected topics* (North Holland, Amsterdam, 1973).
[23] J. Odeurs, Phys. Rev. B **52**(9), 6166 (1995).
[24] R. Coussement, M. van den Bergh, G. S'heeren, and P. Boolchand, Hyperfine Int. **71**(1–4), 1487 (1992).
[25] B. Balko, I. W. Kay, J. Nicoll, J. D. Silk, and G. Herling, Hyperfine Int. **107**, 283 (1997).
[26] J. Odeurs and R. Coussement, Hyperfine Int. **107**(1–4), 299 (1997).
[27] D. H. Perkins, *Introduction to high energy physics* (Addison-Wesley, 1987), 3rd ed.
[28] B. Povh, K. Rith, C. Scholz, and F. Zetsche, *Particles and Nuclei: an introduction to the physical concepts* (Springer, 2008), sixth ed.
[29] W. Grimus and P. Stockinger, Phys. Rev. **D54**, 3414 (1996), hep-ph/9603430.
[30] P. Meystre and M. Sargent, *Elements of quantum optics; 4th ed.* (Springer, Berlin, 2007).
[31] L. A. Mikaelyan, V. G. Tsinoev, and A. A. Borovoi, Yad. Fiz. **6**(2), 349 (1967).
[32] K. Kiers, S. Nussinov, and N. Weiss, Phys. Rev. **D53**, 537 (1996), hep-ph/9506271.
[33] C. Giunti, C. W. Kim, and U. W. Lee, Phys. Lett. **B274**, 87 (1992).
[34] C. Giunti and C. W. Kim, Phys. Rev. **D58**, 017301 (1998), hep-ph/9711363.
[35] C. Giunti, Physica Scripta **67**, 29 (2003), hep-ph/0202063.
[36] C. Giunti, C. W. Kim, and U. W. Lee, Phys. Rev. **D44**, 3635 (1991).
[37] C. Giunti, Found. Phys. Lett. **17**, 103 (2004), hep-ph/0302026.
[38] H. Frauenfelder, *The Mössbauer effect* (W. A. Benjamin Inc., New York, 1962).
[39] W. Potzel, private communication.
[40] M. Beuthe, Phys. Rept. **375**, 105 (2003), hep-ph/0109119.